PHYSICAL REVIEW B **77**, 081403(R) (2008)

Theory of snake states in graphene

L. Oroszlány,[2] P. Rakyta,[1] A. Kormányos,[2] C. J. Lambert,[2] and J. Cserti[1]
[1]*Department of Physics of Complex Systems, Eötvös University, H-1117 Budapest, Pázmány Péter sétány 1/A, Hungary*
[2]*Department of Physics, Lancaster University, Lancaster LA1 4YB, United Kingdom*
(Received 6 August 2007; revised manuscript received 19 December 2007; published 12 February 2008)

We study the dynamics of the electrons in a nonuniform magnetic field applied perpendicular to a graphene sheet in the low-energy limit when the excitation states can be described by a Dirac-type Hamiltonian. Compared to two-dimensional electron gas systems, we show that snake states in graphene exhibit peculiar properties related to the underlying dynamics of the Dirac fermions. The current carried by snake states is locally uncompensated, leading to a current inhomogeneity in the ground state.

DOI: 10.1103/PhysRevB.77.081403 PACS number(s): 81.05.Uw, 73.21.−b, 73.43.Cd, 73.63.Nm

In recent experiments on graphene, new transport phenomena resulting from massless Dirac fermion type excitations have been observed, generating huge interest both experimentally and theoretically.[1–3] For reviews on graphene, see Refs. 4–6 and the special issue in Ref. 7.

While a number of experimental and theoretical works have been devoted to elucidating the excitation spectrum and transport properties of conventional two-dimensional electron gases (2DEGs) in nonuniform magnetic fields, very little is known about graphene. For example, in a nonuniform magnetic field 2DEGs are known to possess special states called "snake states" at the boundary where the direction of the magnetic field changes. Snake states in conventional 2DEGs were first studied theoretically by Müller[8] and have inspired numerous theoretical and experimental works (see, e.g., Ref. 9 and references therein). The effect of an inhomogeneous magnetic field on electrons has been much less investigated in graphene. Martino *et al.* have demonstrated that the massless Dirac electron can be confined in an inhomogeneous magnetic field.[10] Tahir and Sabeeh have studied the magnetoconductivity of graphene in a spatially modulated magnetic field and shown that the amplitudes of the Weiss oscillation are larger than those in a 2DEG.[11] The low-energy electronic bands have been studied by Guinea *et al.*,[12] taking into account the nonhomogeneous effective gauge field due to the ripples of the graphene sheet. However, snake states have been studied only in carbon nanotubes very recently by Nemec and Cuniberti[13] and by Lee and Novikov.[14]

In this work we study the excitation spectrum of a graphene nanoribbon in a nonuniform magnetic field as shown in Fig. 1. In particular, we demonstrate the existence of snake states exhibiting peculiar behavior at low energy. We find that these snake states are localized in the zero-magnetic-field region and carry current which is compensated at the edges of the sample far from the central region. For low Fermi energies E_F this leads to a different ground state current distribution than in the case of a 2DEG.

To study snake states in graphene we consider a simple steplike, nonuniform magnetic field applied perpendicular to the graphene sheet, as shown in Fig. 1. We elucidate the nature of these states by obtaining exact solutions of an analytical model and performing numerical tight binding (TB) calculations. We start our discussion by introducing the Dirac equation framework.

The Dirac Hamiltonian of graphene in a low-energy approximation reads $H_{\pm}=v(\sigma_x\pi_x\pm\sigma_y\pi_y)$, where the index $+$ $(-)$ corresponds to the valley $\mathbf{K}$ $(\mathbf{K}')$. The Fermi velocity $v=(\sqrt{3}/2)a\gamma/\hbar$ is given by the coupling constant γ between the nearest neighbors in graphene ($a=0.246$ nm is the lattice constant in the honeycomb lattice), while $\boldsymbol{\pi}=(\pi_x,\pi_y)=\mathbf{p}-e\mathbf{A}$, where $\mathbf{p}$ is the canonical momentum and the vector potential $\mathbf{A}$ is related to the magnetic field through $\mathbf{B}=\mathrm{rot}\mathbf{A}$. The Pauli matrices σ_x and σ_y act in the pseudospin space. The Hamiltonian is valley degenerate for arbitrary magnetic field, i.e., $\sigma_x H_{\pm}\sigma_x=H_{\mp}$, therefore it is enough to consider only one valley; in what follows we take valley $\mathbf{K}$.

The energy spectrum of our system can be obtained from the Schrödinger equation $H_+\Psi(x,y)=E\Psi(x,y)$. To construct the wave function in each region we utilize the symmetries of the system. The translational invariance in the $\hat{y}$ direction implies that $[H,p_y]=0$ in the Landau gauge if the vector potential is given by $\mathbf{A}=(0,A_y(x),0)^T$. Therefore the wave function can be separated: $\Psi(x,y)=\Phi(x)e^{iky}$, where k is the wave number along the $\hat{y}$ direction (measured from the $\mathbf{K}$ point of the Brillouin zone). One can also show that

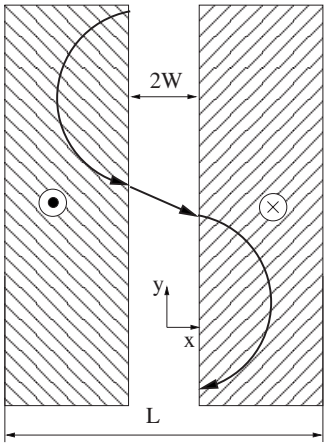

FIG. 1. The magnetic field applied perpendicular to the graphene is zero in the center region of width $2W$, while in the left and right regions the magnetic fields point in opposite directions with the same magnitude B. The total width of the strip is $L\gg W$. The classical trajectory of a typical snake state is also drawn schematically.

$[H,\sigma_y T_x]=0$, where T_x is the reflection operator, i.e., it acts on an arbitrary function $f(x)$ as $T_x f(x)=f(-x)$. This means that the wave functions $\Phi(x)$ can be classified as even wave functions satisfying $\sigma_y T_x \Phi^{(e)}(x)=\Phi^{(e)}(x)$ and odd functions, when $\sigma_y T_x \Phi^{(o)}(x)=-\Phi^{(o)}(x)$. Moreover, it is true that $[\sigma_y T_x, p_y]=0$. From these commutation relations the even (odd) wave function *Ansätze* in the three different regions can be constructed. In the central region, i.e., for $|x| \leqslant W$, and at energy E it is given by

$$\Phi_C^{(e)}(x) = c_1 \left[\begin{pmatrix} 1 \\ e^{i\varphi} \end{pmatrix} e^{iKx} - i \begin{pmatrix} e^{i\varphi} \\ -1 \end{pmatrix} e^{-iKx} \right], \tag{1a}$$

$$\Phi_C^{(o)}(x) = c_1 \left[\begin{pmatrix} 1 \\ e^{i\varphi} \end{pmatrix} e^{iKx} + i \begin{pmatrix} e^{i\varphi} \\ -1 \end{pmatrix} e^{-iKx} \right], \tag{1b}$$

where $\tan\varphi=k/K$, $K=\sqrt{\varepsilon^2-k^2}$ is the transverse wave number, and $\varepsilon=E/(\hbar v)$. For $k>\varepsilon$ the above given wave number K has to be replaced by $K=-i\sqrt{k^2-\varepsilon^2}$. For $x \leqslant -W$ the wave function in the Landau gauge reads

$$\Phi_L^{(e)}(x) = c_2 \begin{pmatrix} U(a_+,\xi) \\ \eta U(a_-,\xi) \end{pmatrix}, \quad \Phi_L^{(o)} = \Phi_L^{(e)}, \tag{1c}$$

where $\xi=-\sqrt{2}(x+W+kl^2)/l$, $l=\sqrt{\hbar/|eB|}$ is the magnetic length, $a_\pm=(\pm 1-\varepsilon^2 l^2)/2$, $\eta=-i\sqrt{2}/(\varepsilon l)$, and $U(a,x)$ is a parabolic cylinder function.[15] Finally, the wave function *Ansatz* in the right region, i.e., for $x \geqslant W$, can be obtained from $\Phi_L^{(e,o)}(x)$ as $\Phi_R^{(e)}(x)=\sigma_y T_x \Phi_L^{(e)}(x)$ and $\Phi_R^{(o)}(x)=-\sigma_y T_x \Phi_L^{(o)}(x)$. Note that in our analytical calculations we assume that $L \gg l$; hence from the two solutions of the parabolic cylinder equation we keep only that one which goes to zero for $x \to \pm\infty$. The boundary conditions require the continuity of the wave function at $x=\pm W$, resulting in a homogeneous system of equations for the amplitudes c_1 and c_2. Nontrivial solutions can be obtained from a secular equation resulting in energy bands $E_n(k)$ labeled by $n=0,\pm 1,\ldots$ for a given k. Owing to the chiral symmetry $(\sigma_z H_\pm \sigma_z=-H_\pm)$ we have $E_{-n}(k)=-E_n(k)$.[16]

Our TB calculations are similar to those made by Wakabayashi *et al.*[18] except that we consider a nonuniform magnetic field. The band structure $E_n(\tilde{k})$, assuming periodic boundary conditions in the $\hat{y}$ direction and zigzag edges at $x=\pm L/2$, is shown in Fig. 2 for all allowed $\tilde{k}$. The energies are scaled in units of $\hbar\omega_c$, where $\hbar\omega_c=\sqrt{2}\hbar v/l=\sqrt{3/2}\gamma a/l$. As shown in Fig. 3, around the **K** point, where the Dirac equation is expected to be valid, the TB calculations are also in excellent agreement with the results from our analytical calculations.

One can see in Fig. 3 that for large enough positive k, each state evolves into dispersionless, twofold-degenerate Landau-level-like states having in very good approximation the same energies as in the case of uniform magnetic field, i.e., $E_n^L=\mathrm{sgn}(n)\hbar\omega_c\sqrt{|n|}$ with $n=0,\pm 1,\ldots$, where $\mathrm{sgn}(\cdot)$ is the sign function (see, e.g., Refs. 16 and 19). (Nevertheless, as can be observed in Fig. 2, for even greater k, i.e., far from the **K** point, when the guiding center coordinate kl^2 of these states is close to the edge of the nanoribbon, they acquire

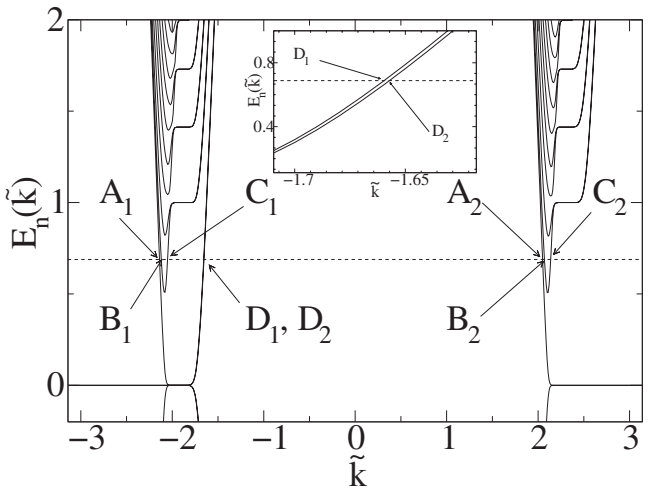

FIG. 2. Dispersion relation $E_n(\tilde{k})$ (the energy is in units of $\hbar\omega_c$, while $\tilde{k}$ is in $1/a$). (For clarity, we have also included a small portion of the valence bands.) The strength of the magnetic field corresponds to $W/l=2.2$; for other parameters see Ref. 17. At the energy indicated by the dashed line there are eight states: A_i, B_i, C_i, and D_i with $i=1,2$ (see the text). The inset shows an enlargement of the band structure for this energy with the states $D_{1,2}$.

dispersion.) For negative values of k, however, the energy bands are already dispersive close to the **K** point. Examples for such states are A_1, B_1, and C_1 in Figs. 2 and 3. Each of these states carries current in the $\hat{y}$ or $-\hat{y}$ direction depending on their group velocity. The corresponding wave functions and the current carried by them are localized in the central, zero-magnetic-field region. This is shown in Fig. 4, where the current distribution of states A_1, B_1, and C_1 at the energy indicated by the dashed line in Fig. 2 can be seen. States A_i, B_i, and C_i are therefore the snake states in our system.

Moreover, comparing Figs. 2 and 3, one can observe that far from the **K** point there are another two dispersive, current-carrying states, denoted by $D_{1,2}$ in Fig. 2. These states are surface states localized close to the edges

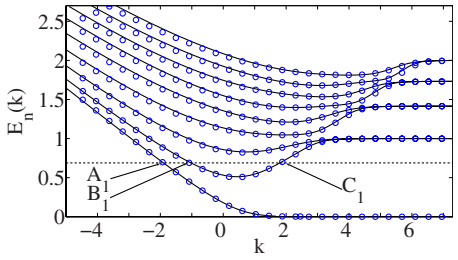

FIG. 3. (Color online) Energy bands $E_n(k)$ (in units of $\hbar\omega_c$) as a function of k (in units of $1/W$) around the **K** point for magnetic field corresponding to $W/l=2.2$. The solid lines (open circles) are the results obtained from the Dirac equation (TB model). Only the conduction band $[E_n(k) \geqslant 0]$ with $n=0,1,\ldots,8$ states is shown ($n=0$ corresponds to the lowest conduction subband, and the other bands are in increasing order of energy). The even (odd) wave function states correspond to even (odd) quantum number n. States A_1, B_1, and C_1 at energy $0.688\hbar\omega_c$ (dotted line) are snake states (see the text).

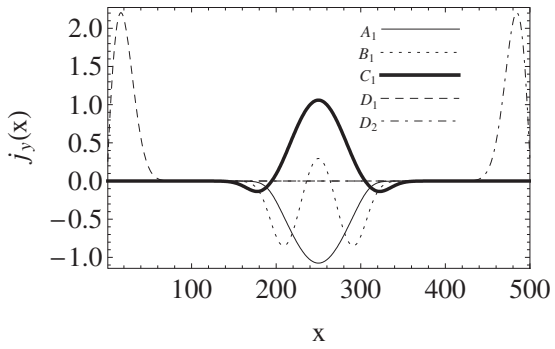

FIG. 4. Current density $j_y(x)$ (in arbitrary units) as a function of x (in units of lattice site x ranging from 1 to N) for states A_1, B_1, C_1, D_1, and D_2 shown in Fig. 2. The zero-magnetic-field region is between site indices $x=200$ and 300.

$(x=\pm L/2)$ of the system, which is also reflected in the corresponding current densities shown in Fig. 4.

We now show that for low enough Fermi energies the above discussed properties of the snake and edge states result in a characteristic ground state current distribution, which is different from what one can find in 2DEGs. By adding up all the current contributions from states below and at Fermi energy $E_F=0.688\hbar\omega_c$, the calculated ground state current density as a function of the cross section coordinate x can be seen in Fig. 5(a). Integrating the current density in a stripe of width of $\approx 2(W+l)$ in the middle of the sample, we find that there is a net current flowing in the $-\hat{y}$ direction. {Since $J(x)$ is basically zero far from the edges of the system and from the zero-magnetic-field region [see Fig. 5(a)], this finding does not depend on the precise choice of the limits of the integration.} The current flowing in the middle is balanced by currents flowing in the $\hat{y}$ direction close to the edges of the system, so the total current is zero, as required by charge conservation. The origin of this ground state current inhomogenity can be understood in the following way: at each energy there is a locally uncompensated current flowing in the middle region, which adds up from the contributions of the snake states. For example, looking at the states at the

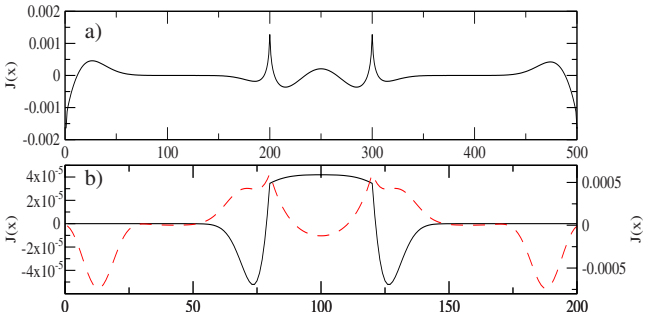

FIG. 5. (Color online) Ground state current density $J_y(x)$ (in arbitrary units) as a function of x (in units of lattice site x ranging from 1 to N). (a) For graphene, for $E_F=0.688\hbar\omega_c$ (indicated by the dashed line in Figs. 2 and 3). The zero-magnetic-field region is between site indices $x=200$ and 300. (b) For a 2DEG if $E_F=0.2\hbar\omega_c$ (black line) and if $E_F=0.6\hbar\omega_c$ [red (gray) dashed line]. The zero-magnetic-field region is between site indices $x=80$ and $x=120$.

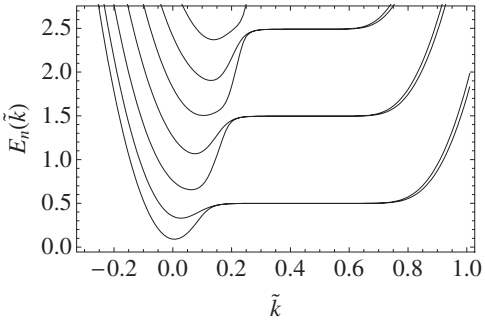

FIG. 6. Energy bands $E_n(\tilde{k})$ of a 2DEG obtained from the TB model for the same magnetic field profile as in Fig. 1 and with magnetic strength as in Fig. 3. The energies are in units of $\hbar\Omega_c$, where $\Omega_c=eB/m$ with effective mass m of electrons, and k is in units of $1/a$, where a is the lattice constant in the square lattice. Here $W=L/10$ and $L=200a$.

Fermi energy, when E_F lies between the first and second Landau levels, i.e., for $E_0^L<E_F<E_1^L$, even though currents from states like B_1 and C_1 compensate each other (see Fig. 4), there is always at least one such snake state, e.g., A_1, whose current is locally, in the middle region, not compensated. Nevertheless, the current balance in the sample is restored by the contributions from surface states like $D_{1,2}$. When the Fermi energy crosses the $n=1$ Landau level then not just states like A_1 but also those like B_1 become uncompensated, because state C_1 evolves into a surface state. It is easy to see from Fig. 2 that in graphene for all $E>0$ there is always at least one locally uncompensated snake state, localized at the center of the sample, and its current is compensated only by surface states far from the center part of the system. This current inhomogeneity is also reflected in the ground state current density.

It is instructive to compare these results with those that one can obtain for 2DEGs for the same magnetic field profile. The energy bands of 2DEG are shown in Fig. 6. For a range of $\tilde{k}$ values, dispersionless Landau levels can be found at energies $E_n^L=\hbar\Omega_c(n+1/2)$, where $n=0,1,\ldots$, as in the case of a uniform magnetic field. Moreover, a similar analysis as for graphene shows that one can find snake[20] and surface states as well. However, the dispersion relation implies that in a 2DEG no locally uncompensated current appears below the first Landau level ($n=0$). This is an important difference between the two systems. Above the $n=0$ Landau level, however, the situation becomes similar to the graphene case: at each energy, the current flowing in the central part of the system (due to the snake states) is compensated by the current carried by the edge states. Indeed, looking at the ground state current distribution shown in Fig. 5(b) with a black line, one can observe that for low Fermi energies $E_F<E_0^L$ the ground state current flows in the central part of the system (although not entirely in the zero-magnetic-field strip) and there is no contribution from states localized close to the edges. In contrast, if the Fermi energy is higher, $E_F>E_0^L$, the ground state current distribution is nonzero both in the middle of the system and close to the edges [shown by the dashed red (gray) line in Fig. 5(b)], and the net current flowing in the middle is offset by currents flowing at the edges, just as in the graphene case.

In summary, we have studied the dynamics of electrons in graphene in a nonuniform perpendicular magnetic field. We calculated the energy bands in the case of an infinite system using the Dirac Hamiltonian, and the results agree very well with those obtained from our TB calculations. For a simple, steplike magnetic field profile we have shown that, at any particular energy, snake states appear carrying locally uncompensated currents and surface states localized at the edges of the sample ensure a non-current-carrying ground state. This current inhomogeneity is, moreover, also reflected in the ground state current distribution. In 2DEGs, on the other hand, we find that, for Fermi energies below the energy of the first Landau level, the ground state current is confined to the central region of the sample, because there are no surface states. Therefore the existence of locally uncompensated snake states at all energies and the ground state current inhomogeneity for low Fermi energies are clear manifestations of the massless Dirac-fermion-like excitations. By analogy with the quantum Hall effect, the snake states for Fermi energies between the Landau level $n=0$ and $n=1$ or $n=-1$ are expected to be resilient against scattering by impurities.

Recently, we have become aware of a paper by Ghosh *et al.*,[21] in which several of the results presented here were also reported.

We acknowledge discussions with E. McCann, V. Fal'ko, F. Guinea, and H. Schomerus. This work is supported partially by European Commission Contract No. MRTN-CT-2003-504574 and EPSRC.

[1] K. S. Novoselov, A. K. Geim, S. V. Morozov, D. Jiang, Y. Zhang, S. V. Dubonos, I. V. Grigorieva, and A. A. Firsov, Science **306**, 666 (2004); K. S. Novoselov, A. K. Geim, S. V. Morozov, D. Jiang, M. I. Katsnelson, I. V. Grigorieva, S. V. Dubonos, and A. A. Firsov, Nature (London) **438**, 197 (2005).

[2] Y. Zhang, J. P. Small, M. E. S. Amori, and P. Kim, Phys. Rev. Lett. **94**, 176803 (2005); Y. Zhang, Y.-W. Tan, H. L. Stormer, and P. Kim, Nature (London) **438**, 201 (2005).

[3] K. S. Novoselov, E. McCann, S. V. Morozov, V. I. Fal'ko, M. I. Katsnelson, U. Zeitler, D. Jiang, F. Schedin, and A. K. Geim, Nat. Phys. **2**, 177 (2006).

[4] M. I. Katsnelson, Mater. Today **10**, 20 (2007).

[5] M. I. Katsnelson and K. S. Novoselov, Solid State Commun. **143**, 3 (2007).

[6] A. K. Geim and K. S. Novoselov, Nat. Mater. **6**, 183 (2007).

[7] Solid State Commun. **143**, 1 (2007), special issue on graphene.

[8] J. E. Müller, Phys. Rev. Lett. **68**, 385 (1992).

[9] J. Reijniers and F. M. Peeters, J. Phys.: Condens. Matter **12**, 9771 (2000); J. Reijniers, A. Matulis, K. Chang, F. M. Peeters, and P. Vasilopoulos, Europhys. Lett. **59**, 749 (2002); H. Xu, T. Heinzel, M. Evaldsson, S. Ihnatsenka, and I. V. Zozoulenko, Phys. Rev. B **75**, 205301 (2007).

[10] A. De Martino, L. Dell'Anna, and R. Egger, Phys. Rev. Lett. **98**, 066802 (2007).

[11] M. Tahir and K. Sabeeh, Phys. Rev. B **76**, 195416 (2007).

[12] F. Guinea, M. I. Katsnelson, and M. A. H. Vozmediano, arXiv:0707.0682 (unpublished).

[13] N. Nemec and G. Cuniberti, Phys. Rev. B **74**, 165411 (2006).

[14] H. W. Lee and D. S. Novikov, Phys. Rev. B **68**, 155402 (2003).

[15] *Handbook of Mathematical Functions*, edited by M. Abramowitz and I. A. Stegun (Dover Publications, New York, 1970).

[16] M. Ezawa, J. Phys. Soc. Jpn. **76**, 094701 (2007).

[17] Only nearest neighbor hopping was considered and the magnetic field is taken into account by the usual Peierls substitution. In our numerical calculations, we used $N=500$ lattice sites in the x direction [thus the width of the graphene ribbon is given by $L=(\sqrt{3}N/2-1)a$] and kept the ratio $W=L/10$ fixed.

[18] K. Wakabayashi, M. Fujita, H. Ajiki, and M. Sigrist, Phys. Rev. B **59**, 8271 (1999).

[19] F. D. M. Haldane, Phys. Rev. Lett. **61**, 2015 (1988); Y. Zheng and T. Ando, Phys. Rev. B **65**, 245420 (2002); V. P. Gusynin and S. G. Sharapov, Phys. Rev. Lett. **95**, 146801 (2005); N. M. R. Peres, F. Guinea, and A. H. Castro Neto, Phys. Rev. B **73**, 125411 (2006); L. Brey and H. A. Fertig, *ibid.* **73**, 235411 (2006).

[20] In particular, see, e.g., Reijniers and Peeters in Ref. 9.

[21] T. K. Ghosh, A. De Martino, W. Häusler, L. Dell'Anna, and R. Egger, following paper, Phys. Rev. B **77**, 081404(R) (2008).